ELSEVIER

Materials Science and Engineering A 380 (2004) 290–297

MATERIALS SCIENCE & ENGINEERING A

www.elsevier.com/locate/msea

Marangoni convection and weld shape variations in Ar–O_2 and Ar–CO_2 shielded GTA welding

Shanping Lu [a,b,*], Hidetoshi Fujii [a], Kiyoshi Nogi [a]

[a] *Joining and Welding Research Institute, Osaka University, 11-1 Mihogaoka, Ibaraki, Osaka 567-0047, Japan*
[b] *Institute of Metal Research, Chinese Academy of Sciences, 72 Wenhua Road, Shenyang 110016, PR China*

Received 8 December 2003; received in revised form 25 March 2004

Abstract

Increasing the oxygen or the carbon dioxide concentration in the argon-based shielding gas leads to an increase in the weld metal oxygen content when the oxygen or carbon dioxide concentration is to be lower than 0.6 vol.% in the shielding gas. However, when the O_2 or CO_2 concentration is higher than 0.6 vol.% in the Ar-based shielding gas, the weld metal oxygen is maintained around 200 ppm–250 ppm. An inward Marangoni convection mode in the weld pool occurs when the weld metal oxygen content is more than 100 ppm. When it is lower than 100 ppm, the Marangoni convection would change to the outward direction and the weld shape varies from a deep narrow to a shallow wide shape. The effective ranges of O_2 and CO_2 concentrations for deep penetration are same. A heavy layer of oxides is formed when the O_2 or CO_2 concentration in the shielding gas is more than 0.6 vol.%. Based on the thermodynamic calculation of the equilibrium reactions of Fe, Si, Cr and Mn with oxygen in liquid iron for the oxide products, FeO, SiO_2, Cr_2O_3 and MnO and the experimental oxygen content in the weld metal, Cr_2O_3 and SiO_2 oxides are possibly formed at the periphery area of the liquid pool surface under the arc column during the welding process. One model is proposed to illustrate the role of the oxide layer on the Marangoni convection on the pool surface at elevated temperature. The heavy oxide layer inhibited the fluid flow induced by the Marangoni convection and also became a barrier for the oxygen absorption into the molten weld pool.

Keywords: Marangoni convection; Weld shape; Mixed shielding gas; Oxide layer

1. Introduction

Gas tungsten arc (GTA) welding has been widely used in industry especially for stainless steel, titanium alloys and other non-ferrous metals for high quality welds. However, the shallow penetration restricts its ability to weld thicker stainless in a single pass, thus making the productivity relatively low. For the GTA welding, the weld penetration depends to a large extent on the heat transfer mode in the welding pool by convection, which is driven by the electromagnetic force (F_{em}), surface tension (F_γ), buoyancy force (F_b) and impinging force of the arc plasma (F_{arc}) [1]. The surface tension force on the welding pool surface is a principle variable that induces the Marangoni convection in the liquid pool.

Surface-active elements, such as oxygen, sulfur and selenium, can significantly change the temperature coefficient of the surface tension on liquid weld pool surface and the Marangoni convection mode, and ultimately change the weld penetration when their content in the weld pool is over a critical value. Understanding and precisely controlling the effect of the surface-active elements on the weld shape is critical for generating a satisfactory weld joint with deep penetration. After decades of development, there are several ways available to add the surface-active element to the weld pool, such as by composition adjustment of the raw materials [2–6], pre-placing or smearing active flux on the substrate surface (A-TIG) [7–15] and adjusting the shielding gas concentration [16,17]. The flux smearing in A-TIG must be performed before welding and it is also difficulty for the operator to control the effective quantity of the flux used.

Compared to the A-TIG welding, the investigation on the effect of gaseous additions to the argon-based shielding gas on the weld penetration and weld shape is very limited. However, the mixed gas is easily controlled and can be applied

* Corresponding author. Tel.: +81 6 6879 8663; fax: +81 6 6879 8663.
E-mail addresses: shplu@jwri.osaka-u.ac.jp, shplu@imr.ac.cn (S. Lu).

0921-5093/$ – see front matter © 2004 Elsevier B.V. All rights reserved.
doi:10.1016/j.msea.2004.05.057

by automatic GTA welding in industry if the addition gas can increase the weld penetration efficiently.

For GTA welding, the small addition of oxygen or carbon dioxide to the shielding gas provides a significant source of oxygen absorption for the molten weld pool. This study was designed to investigate the effects of O_2 and CO_2 additions to the argon shielding gas on the Marangoni convection in the weld pool and the weld penetration.

2. Experimental procedure

A 10-mm thick SUS304 stainless plate, with sulfur content of 0.0005 wt.% and oxygen content of 0.0038 wt.%, was selected for the bead-on-plate welding experiments. Prior to welding, the surface of the plate was ground in order to remove all scale and was degreased by acetone. The detailed composition of the plate is given in Table 1.

A direct current electrode negative (DCEN) polarity power source was used with a mechanized system in which the test piece was moved at a constant speed under the torch. Bead-on-plate welds were made at the set welding parameters listed in Table 2. The 2% thoriated tungsten electrode was ground and the electrode gap was measured for each new bead before welding to ensure that the bead was made under the same conditions except for the shielding gas concentrations.

To modify the argon-based shielding gas, controlled levels of oxygen or carbon dioxide were added to the argon-based shielding gas. All the O_2–Ar and CO_2–Ar mixtures were prepared from pure argon and a premixed argon 1 vol.%O_2, 0.92 vol.%CO_2 and 20 vol.%CO_2. In the experiments, the O_2 content in the O_2–Ar mixed shielding gas was in the range of 0.1 vol.%–1.0 vol.%. The CO_2 content in CO_2–Ar mixed shielding gas was in the range of 0.092 vol.%–1.0 vol.%.

Table 1
Chemical composition of SUS304 stainless plate

Alloy element	C	Si	Mn	Ni	Cr	P	S	O	Fe
Content (wt.%)	0.06	0.44	0.96	8.19	18.22	0.027	0.0005	0.0038	Bal.

Table 2
Welding parameters

Parameters	Value
Electrode type	DCEN, W–2%ThO_2
Diameter of electrode (mm)	1.6
Vertex angle of electrode (°)	60
Shield gas	O_2–Ar, CO_2–Ar
Gas flow rate (L/min)	10
Electrode gap (mm)	3
Bead length (mm)	50
Spot time (s)	3
Welding current (A)	160
Welding speed (mm/s)	2

Subsequent to welding, samples for the weld shape observations were prepared using the standard metallographic techniques and etched by a $HCl + Cu_2SO_4$ solution to reveal the bead shape and dimensions. The cross-sections of the weld beads were photographed using an optical microscope (Olympus, HC300 Z/OL). At the same time, samples for the weld metal oxygen analysis were directly extracted from the weld fusion zone and measured by oxygen/nitrogen analyzer (Horiba, EMGA-520). The oxide layer on the weld surface was also observed and photographed using a laser microscope (Keyence, VK-8550). The composition analysis to the solidified oxide layer was by EDAX (ESEM-2700).

3. Results and discussion

3.1. Oxygen content in weld metal

The weld metal oxygen content is plotted versus the oxygen and carbon dioxide concentrations in the shielding gas as shown in Fig. 1. As anticipated, the weld metal oxygen content increases with the oxygen or carbon dioxide concentration in the torch shielding gas when the O_2 or CO_2 addition in the argon gas is lower than 0.6 vol.%. However, when the O_2 or CO_2 addition content in argon is over 0.6 vol.%, the weld metal oxygen content is maintained around 200 ppm. The oxygen and carbon dioxide nearly have the same effect on the oxygen absorption for the molten weld metal in the GTA welding process when the O_2 or CO_2 addition concentration in argon is below 1.0 vol.%. The relationship between the weld metal oxygen content and O_2 or CO_2 addition concentration in the argon shielding gas can be expressed by a line regressive analysis using the data in Fig. 1.

$$[O]_{\text{weld metal/ppm}} = 384\{[O_2]\text{or}[CO_2]\}_{\text{shielding gas/vol.\%}} + 2 \quad ([O_2]\text{or}[CO_2] < 0.6\,\text{vol.\%}) \tag{1}$$

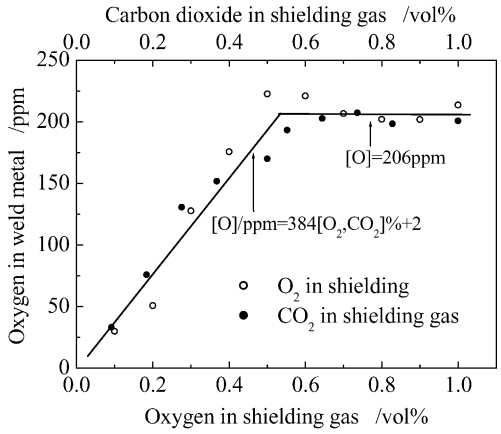

Fig. 1. Weld metal oxygen content as a function of oxygen and carbon dioxide in the shielding gas.

$$[O]_{\text{weld metal/ppm}} = 206 \quad (0.6\,\text{vol.\%} \le [O_2]\text{or}[CO_2] \le 1.0\,\text{vol.\%}) \tag{2}$$

Kuwana and Sato [18–26] have systematically investigated the fundamentals of oxygen absorption under oxidizing gases additions (Ar–O_2, Ar–CO_2 and Ar–O_2–CO_2) metal arc welding (GMAW) for pure iron, Fe–Si, Fe–Mn, Fe–Cr, Fe–Al, Fe–Ti and Fe–Ni steels and tungsten arc welding (GTAW) for pure iron. They found that the weld metal oxygen absorption content under Ar–O_2 is higher than that under Ar–CO_2 shielding gas because the oxidation ability of O_2 is higher than that of CO_2. However, as shown in Fig. 1, the oxygen contents in the weld metal for Ar–O_2 and Ar–CO_2 are nearly the same when the O_2 and CO_2 additions are below 1.0 vol.%, which is different from the findings by Kuwana and Sato. Compared with the experimental conditions by Kuwana and Sato, the oxygen and carbon dioxide contents in the argon shielding gas in our experiments are much lower (0.1 vol.% to 1.0 vol.%) than the ranges in their experiments. Therefore, the weld metal oxygen content is quite low here both for Ar–O_2 and Ar–CO_2 shielding gases, which may be one reason for the quite small different effects of O_2 and CO_2 on the oxygen absorption for weld pool as shown in Fig. 1. However, this low oxygen content value in the weld pool is in the range of the critical value, which can control the Marangoni convection mode on the weld pool surface.

During the GTA welding process, an arc plasma phase resides above the welding pool. Binary or ternary molecular species in the shielding gas are easily dissociated into a monatomic gas and ion in the high temperature plasma column. When the oxygen or carbon dioxide is added to the argon shielding gas, monatomic oxygen gas, O(gas), is produced by the dissociation reactions of $O_2 \rightarrow 2O$ and $CO_2 \rightarrow CO + O$ in the arc plasma column. The monatomic oxygen will dissolve in the welding pool when it moves to the liquid pool surface. Dissociated monatomic O and molecular O_2 or CO_2 are coexisting above the welding pool surface. Therefore, the following representative absorption reactions of oxygen in the weld pool are suggested during the welding process.

For O_2 induced shielding gas:

$$O_2(\text{gas}) = 2O(\text{in liquid pool}) \tag{3}$$

$$O(\text{gas}) = O(\text{in liquid pool}) \tag{4}$$

For CO_2 induced shielding gas:

$$CO_2(\text{gas}) = CO + O(\text{in liquid pool}) \tag{5}$$

$$O(\text{gas}) = O(\text{in liquid pool}) \tag{6}$$

Oxygen absorption in the weld pool not only depends on the partial pressure of O_2 or CO_2, but also on the partial pressure of the monatomic oxygen gas. The total solubility of oxygen in the weld pool is the sum of the absorptions of the oxygen/weld pool and monatomic oxygen/weld pool systems for the O_2 induced shielding gas, and carbon dioxide/weld pool, carbon monoxide/weld pool and monatomic oxygen/weld pool systems for the CO_2 induced shielding gas.

DebRoy and Palmer [27] proposed that the concentration of atomic nitrogen gas from the dissociation of diatomic nitrogen in the plasma is much higher than what would be obtained from the consideration of thermal dissociation of diatomic nitrogen for nitrogen induced shielding gas. The partial pressure of monatomic nitrogen gas is far in excess of what is expected under equilibrium conditions from the thermal dissociation of diatomic nitrogen, and the contribution of diatomic nitrogen is insignificant for the absorption of nitrogen in the liquid metal. Therefore, the partial pressure of the monatomic nitrogen gas plays a more important role in the contribution of the nitrogen absorption in the liquid metal. Many research results [28–33] have shown the importance of monatomic gas for the dissolution in the liquid metal. Since the dissociation reactions of oxygen and carbon dioxide are similar to that of nitrogen in an arc plasma column, it is assumed that the partial pressure of monatomic oxygen in the arc plasma also plays the main role in the absorption of oxygen into the liquid weld pool. The temperature in the arc plasma column above the weld pool is very high, especially close to the electrode area [34]. The dissociation reactions of O_2 and CO_2 significantly occur in the arc plasma column and possibly produce a similar monatomic oxygen gas partial pressure when the oxygen and carbon dioxide contents in the shielding gas are very low. Since it is assumed that the partial pressure of monatomic oxygen gas plays the main role in the absorption of oxygen into the weld pool, the weld metal oxygen content under O_2–Ar shielding gas is nearly the same as that under the CO_2–Ar shielding gas as shown in Fig. 1.

When the O_2 or CO_2 concentration in the shielding gas increases, the O_2 and CO_2 partial pressures and the partial pressure of monatomic oxygen gas will increase from the dissociation reactions of $O_2 \rightarrow 2O$ and $CO_2 \rightarrow CO + O$. The higher the O_2 and CO_2 partial pressures and the partial pressure of monatomic oxygen gas above the weld pool, the more the oxygen dissolves in the weld pool. Therefore, the weld metal oxygen content initially increases with the O_2 or CO_2 concentration in the shielding gas as shown in Fig. 1. However, the dissolution of oxygen in the weld pool is limited in the welding process because the liquid weld pool quickly solidifies in the welding thermal circle as the arc moves away. There is not enough time for the oxygen absorption into the weld pool. Also, the welding pool surface condition is another important factor affecting the oxygen absorption. When the oxygen or carbon dioxide concentration in the shielding gas is over 0.6 vol.%, a heavy oxide layer covers the liquid pool surface as shown in Figs. 5(c and f). This heavy oxide layer is a barrier for oxygen absorption into the welding pool. Under the co-affections of limited dissolution time in the welding process and heavy oxide layer on the pool, the weld metal oxygen content remains

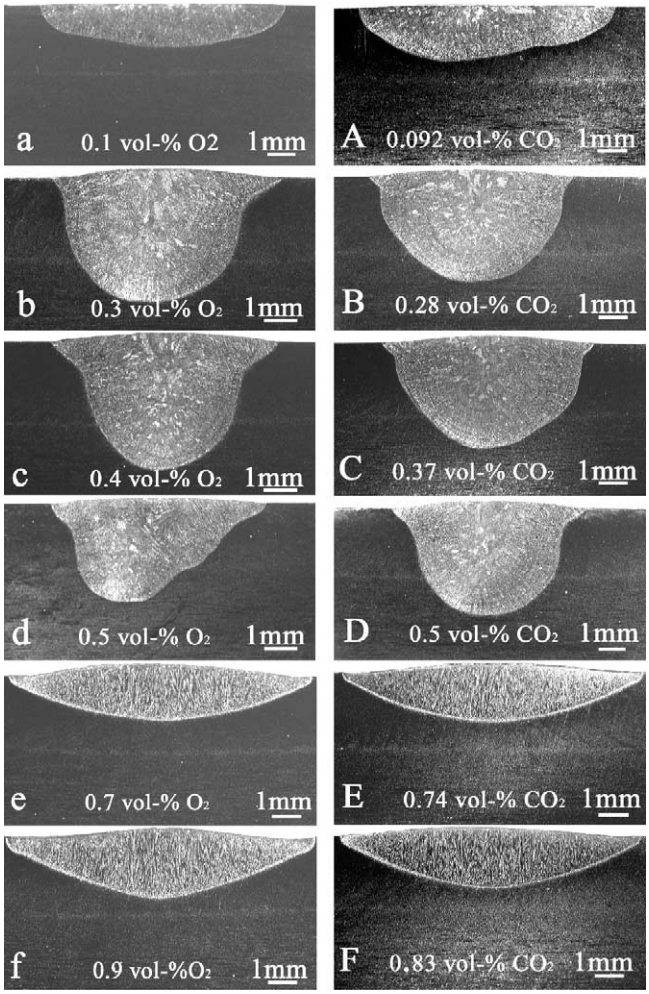

Fig. 2. Weld shapes under different oxygen and carbon dioxide concentrations in argon shielding gas.

nearly constant at around 200 ppm–250 ppm when the O_2 or CO_2 concentration in the shielding gas is over 0.6 vol.% as shown in Fig. 1.

3.2. Weld shape and weld depth/width ratio

Both the O_2 and CO_2 additions to the argon-based shielding gas has a significant effect on the weld pool shape as shown in Fig. 2. The weld depth/width ratio (D/W) is plotted versus the O_2 and CO_2 concentration in the shielding gas in Fig. 3. When the O_2 or CO_2 addition content is below 0.2 vol.%, the weld shape is wide and shallow as shown in Figs. 2(a and A). When the O_2 or CO_2 addition content is over 0.2 vol.% and below 0.6 vol.%, the weld shape becomes deep and narrow as shown in Figs. 2(b–d and B–D). A further increase in the O_2 or CO_2 content in shielding gas leads to shallow and wide weld shape again as shown in Figs. 2(e, f, E and F). It is interesting to note that the weld shape is quite different between low O_2 and CO_2 additions (<0.2 vol.%) and high O_2 or CO_2 additions (>0.6 vol.%) though both of them have wide and shallow weld shapes.

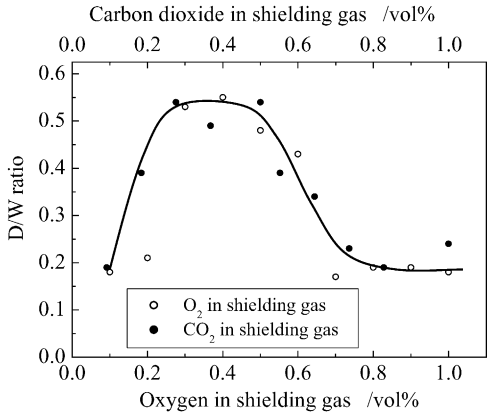

Fig. 3. Weld D/W ratio as a function of oxygen and carbon dioxide in the shielding gas.

The weld pool with low O_2 or CO_2 additions has a flat bottom shape, while weld pools under high O_2 or CO_2 additions have a concave bottom shape. The weld depth/width ratio increases first following by the decrease when the O_2 or CO_2 addition is over 0.6 vol.% as shown in Fig. 3. The weld penetration depths both for the oxygen and carbon dioxide added argon-based shielding gases are dependant to a large extent on the weld metal oxygen content.

3.3. Marangoni convection in weld pool

In GTA welding process, the Marangoni convection mode on the weld pool surface can significantly change the heat transfer behavior in the welding pool, and therefore, change the weld shape. Generally, the surface tension decreases with the increasing temperature, $\partial\sigma/\partial T < 0$, for a pure metal and many alloys. Since there is a large temperature gradient existing on the welding pool surface between the center under the torch and the edges of the weld pool, a large surface tension gradient will be produced along the surface. In the weld pool for such materials, the surface tension is higher in the relatively cooler part of the pool edge than that

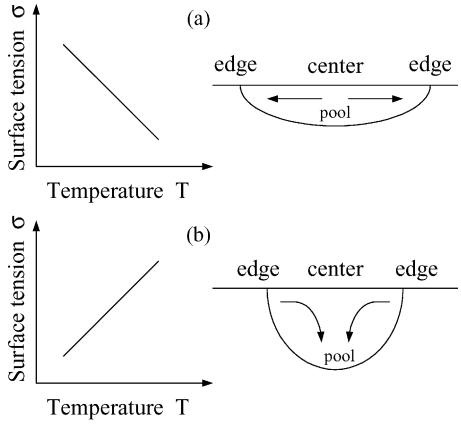

Fig. 4. Schematic of Marangoni convection mode in welding pool.

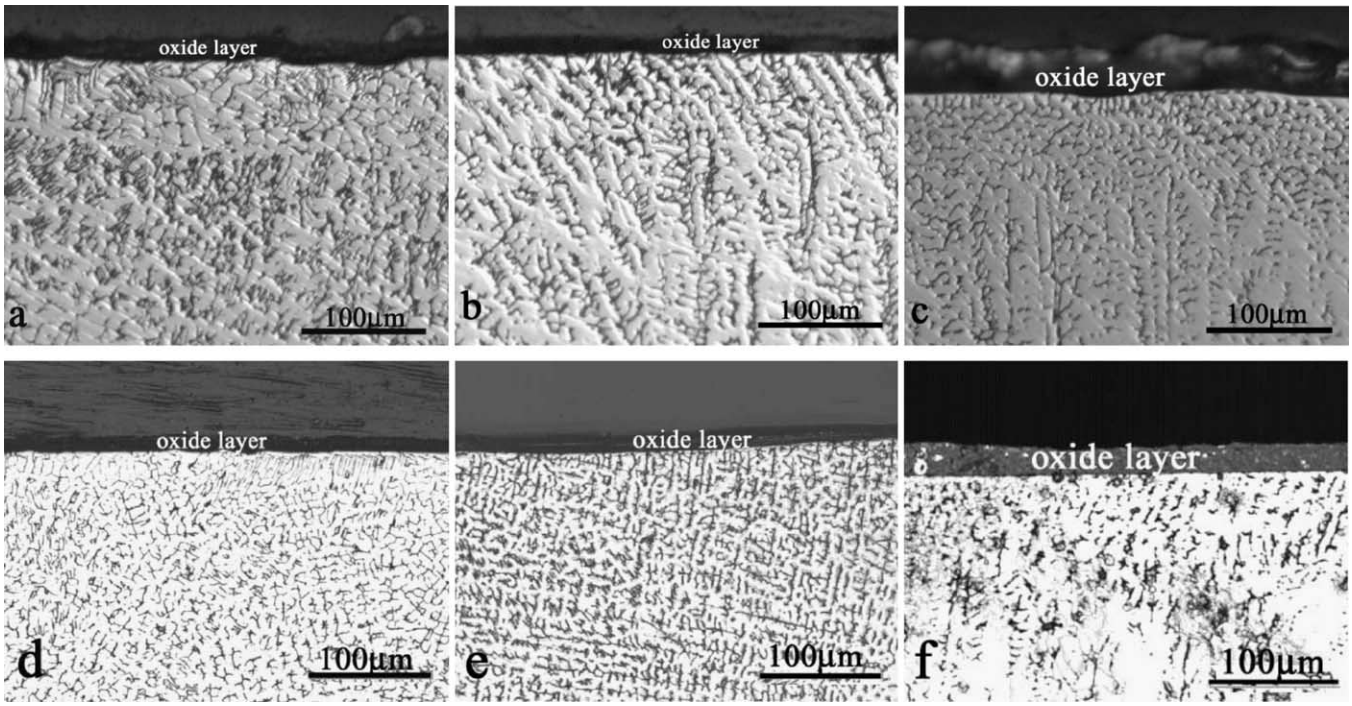

Fig. 5. Oxide layer on weld surface with different oxygen and carbon dioxide concentrations in argon shielding gas.

in the pool center under the arc, and hence, the fluid flows from the pool center to the edge. In that case, the heat flux is easily transferred from the center to the edges and the weld shape is relatively wide and shallow as shown in Fig. 4(a). When the surface-active elements, such as sulfur, oxygen or selenium, exceed a certain concentration in a stainless steel weld metal [5,10], the temperature coefficient of the surface tension changes from a negative to positive value, $\partial\sigma/\partial T > 0$, and the direction of the Marangoni convection in the weld pool changes as illustrated in Fig. 4(b). In this case, a relatively deep and narrow weld is made.

Decomposition of CO_2 and O_2 in the shielding gas provides a significant source of oxygen absorption for the molten weld in the GTA welding process. Fig. 1 shows that the weld metal oxygen content increases with the CO_2 and O_2 concentration in shielding gas when the O_2 and CO_2 content is below 0.6 vol.%. Former research has shown that oxygen is an active element in pure iron and stainless steel in the range of 150 ppm–350 ppm [35] and 70 ppm–300 ppm [36], respectively. In these ranges, the temperature coefficient of surface tension of the welding pool is positive, and inward Marangoni convection occurs in the liquid pool as shown in Fig. 4(b). Below this range, the temperature coefficient of the surface tension becomes negative. Experimental results here agree with the former research. When the O_2 or CO_2 addition content in the shielding gas is over 0.2 vol.%, the weld metal oxygen content is over 100 ppm as shown in Fig. 1, and hence the weld pool Marnagoni convection model suddenly changes from outward to inward. The weld shapes change from shallow wide to deep narrow as shown in Fig. 2. The critical volume concentration of the O_2 and CO_2 addition in the shielding gas is 0.2 vol.%. It is interesting to find that the weld metal oxygen content remains nearly constant around 200 ppm when the O_2 or CO_2 concentration in the shielding gas is between 0.6 vol.% and 1.0 vol.%. However, the weld D/W ratio decreases again as shown in Fig. 3.

3.4. Oxide layer on weld pool surface

The addition of oxygen or carbon dioxide to the argon shielding possibly made the oxidation of the liquid weld pool surface. Fig. 5 shows the solidified oxide layer on the weld surface. The oxide layer on the weld is at 10 μm as shown in Figs. 5(a, b, d and e) when the O_2 or CO_2 addition concentration is lower than 0.6 vol.%. When the O_2 or CO_2 addition is more than 0.6 vol.%, a heavy oxide layer around 30 μm forms on the pool surface as shown in Figs. 5(c and f). This heavy oxide layer plays an important role as a barrier for oxygen absorption into the molten pool and inhibits the Marangoni convection induced by the surface tension of the liquid pool.

The analyzed composition results of the solidified oxide layer are given in Table 3. The solidified oxide layer possibly generated during both the welding process on liquid pool and the solidification process of the pool. However, the oxide type and behavior on the liquid pool under arc column play an important role in the Marangoni convection of the liquid pool. Thermodynamic calculations of the reactions for the oxides formation are estimated under the assumption that the weld pool is considered as an Fe–M–O system. The equilibrium reactions of Fe, Si, Cr and Mn with oxygen in

Table 3
Compositions of the solidified heavy oxide layer (%)

Shielding gas	O	Mn	Fe	Cr	Si	Al
Ar–0.70%O_2	32.5	23.1	7.3	13.7	22.4	1.0
	28.4	24.3	9.9	12.8	23.5	1.1
Ar–0.90%O_2	37.4	16.6	10.4	9.5	23.7	2.4
	33.7	17.0	10.8	12.9	24.1	1.4
Ar–0.60%CO_2	33.3	11.1	10.0	23.5	21.1	1.0
	30.1	11.7	10.7	32.9	13.7	1.0
Ar–0.74%CO_2	29.8	16.4	11.3	22.7	18.6	1.3
	31.1	12.9	9.0	25.0	21.0	1.1

the liquid iron for the oxide products, FeO, SiO_2, Cr_2O_3 and MnO are given by the following equations, respectively [18,20,21,25].

For the Fe–O system:

$$\mathrm{FeO(l)} = \mathrm{Fe(l)} + \underline{\mathrm{O}} \tag{7a}$$

$$\log K' = \log L_o = \frac{\log[\%\mathrm{O}]}{a_{\mathrm{FeO}}} = -\frac{6320}{T} + 2.734 \tag{7b}$$

$$1/2\mathrm{O_2(g)} = \underline{\mathrm{O}} \tag{8a}$$

$$\log K_{\mathrm{O}} = \frac{\log[\%\mathrm{O}]}{P_{\mathrm{O_2}}^{1/2}} = \frac{6104}{T} + 0.12 \tag{8b}$$

where [%O] is the oxygen content in the weld pool; and a_{FeO} is the activity of FeO. When the FeO is separated out, a_{FeO} can be set to 1. $P_{\mathrm{O_2}}$ is the oxygen partial pressure.

For the Fe–Si–O system:

$$\mathrm{SiO_2(s)} = \mathrm{Si(l)} + 2\underline{\mathrm{O}} \tag{9a}$$

$$\log K = \log a_{\mathrm{Si}} a_{\mathrm{o}}^2 = -\frac{30110}{T} + 11.40 \tag{9b}$$

where a_{Si} and a_{o} are the activities of the Si and O, respectively. If introducing K' using the mass% silicon and oxygen instead of K, the following equation is obtained:

$$\log K' = \log[\%\mathrm{Si}][\%\mathrm{O}]^2 = \frac{-30410}{T} + 11.59 \tag{9c}$$

For the Fe–Cr–O system:

$$\mathrm{Cr_2O_3(s)} = 2\mathrm{Cr} + 3\underline{\mathrm{O}} \tag{10a}$$

$$\log K = \log a_{\mathrm{Cr}}^2 a_{\mathrm{o}}^3 = \frac{-44040}{T} + 19.42 \tag{10b}$$

where a_{Cr} and a_{o} are the activities of the Cr and O, respectively. If introducing K' using the mass% chromium and oxygen instead of K, the following equation is obtained:

$$\log K' = \log[\%\mathrm{Cr}]^2[\%\mathrm{O}]^3 = \frac{-44040}{T} + 19.42 \tag{10c}$$

For the Fe–Mn–O system:

$$\mathrm{FeO(l)} + \underline{\mathrm{Mn}} = \mathrm{MnO(l)} + \mathrm{Fe(l)} \tag{11a}$$

$$\log K_{\mathrm{Mn}} = \frac{\log a_{\mathrm{MnO}}}{a_{\mathrm{FeO}} a_{\mathrm{Mn}}} = \frac{6440}{T} - 2.95 \tag{11b}$$

where a_{MnO}, a_{FeO} and a_{Mn} are the activities of MnO in FeO–MnO, FeO in FeO–MnO and Mn in the liquid iron, respectively. Assuming that the oxygen and manganese activity coefficients in the liquid iron are 1, following equation is derived

$$[\%\mathrm{O}] = \frac{L_o}{(1 + K_{\mathrm{Mn}}(\%\mathrm{Mn}))} \tag{11c}$$

where L_{o} is oxygen distribution coefficient between the liquid iron and FeO, as shown in Eq. (7b).

Using Eqs. (7–11), the equilibrium oxygen content in the liquid iron and the oxygen partial pressure are calculated and shown in Table 4 under 1773 K, 1873 K and 2273 K, respectively. For FeO and MnO oxide formation reactions (Eqs. (7–11)), the equilibrium oxygen contents in liquid pool are higher than that for the SiO_2 and Cr_2O_3 oxide formation reactions (Eqs. (9) and (10)) as shown in Table 4. The oxygen analysis of the weld metal showed that the oxygen content in the weld metal is between 30 ppm and 250 ppm as shown in Fig. 1, which is lower than the values of the calculated equilibrium oxygen content for the FeO and MnO oxide formation reactions as shown in Table 4. In the moving GTA welding process, the dissolution of the oxygen in the liquid pool is a non-equilibrium process, and thereby, the oxygen content in the weld metal is low. However, for the SiO_2 and Cr_2O_3 oxide formation reactions (Eqs. (9) and (10)), the calculated equilibrium oxygen contents in the liquid iron are very low, 0.0025% (25 ppm) and 0.0023% (23 ppm) under 1773 K, and 0.0072% (72 ppm) and 0.0062% (62 ppm) under 1873 K as shown in Table 4, which are lower than the experimental values of the oxygen content in the weld metal. Therefore, the SiO_2 and Cr_2O_3 oxides are possibly formed on the liquid pool surface. However, when the temperature is increased to 2273 K, the calculated equilibrium oxygen contents for the SiO_2 formation reaction (Eq. (9)) and Cr_2O_3

Table 4
Equilibrium oxygen content and oxygen partial pressure by thermodynamic calculations

Oxides	Equilibrium oxygen content [%O]			Equilibrium oxygen partial pressure (atm)		
	1773 K	1873 K	2273 K	1773 K	1873 K	2273 K
FeO	0.1477	0.2289	0.8985	1.6×10^{-9}	9.2×10^{-9}	2.0×10^{-6}
SiO_2	0.0025	0.0072	0.1922	4.7×10^{-13}	9.0×10^{-12}	9.1×10^{-8}
Cr_2O_3	0.0023	0.0062	0.1495	3.8×10^{-13}	6.8×10^{-12}	5.5×10^{-8}
MnO	0.0263	0.0570	0.5122	5.2×10^{-11}	5.9×10^{-10}	6.4×10^{-7}

formation reaction (Eq. (10)) are 0.1922% (1922 ppm) and 0.1495% (1495 ppm), respectively, which are much higher than the experimental values of the weld metal oxygen content. Therefore, the SiO_2 and Cr_2O_3 may not generate at high temperature. In the moving GTA welding with a weld current of 150 A, and a weld speed of 2.5 mm/s, the peak temperature of the weld pool center is between 2200 K and 2500 K for SUS304 stainless steel [37]. In the experiments here, the welding current is 160 A and the welding speed is 2.0 mm/s as shown in Table 2. The peak temperature of the pool should be in the range of 2200 K–2500 K. For this case, the solid Cr_2O_3 (melting point: 2538 K) and SiO_2 (melting point: 2001 K) oxides should form at the periphery area on the weld pool surface, where the temperature is relatively low. In the liquid pool center area, the temperature is high and Cr_2O_3 and SiO_2 oxides will not generate.

One model to illustrate the oxide behavior on the pool surface at elevated temperature is proposed in Fig. 6. When the O_2 or CO_2 addition is below 0.6 vol.%, the oxide layer is thin. This thin oxide layer on the pool periphery area is easily destroyed and exposes the weld pool surface to the arc and shielding gas since the welding pool surface is not stationary and flows under the plasma shear force and surface tension force. Therefore, the oxygen decomposed from CO_2 or O_2 is easily absorbed and dissolved in the welding pool as shown in Fig. 6(a) and (b). When the O_2 or CO_2 addition content is below 0.2 vol.%, the oxygen in weld pool is below 100 ppm as shown in Fig. 1, and the Marangoni convection is outward as shown in Fig. 6(a), namely, a quasi-free pool surface with an outward Marangoni convection. Therefore, the weld shape is wide and shallow. When the O_2 or CO_2 is over 0.2 vol.%, the weld metal oxygen content is more than 100 ppm, and the Marangoni convection changes from outward to inward shown in Fig. 6(b), namely, a quasi-free pool surface with an inward convection. In this case, the weld shape is deep and narrow. With a further increase in the O_2 or CO_2 concentration over 0.6 vol.% in the shielding gas, a thick oxide layer forms at periphery area on the liquid pool surface like Fig. 6(c), namely, a restricted pool surface. This continuous thick oxide layer becomes a barrier for oxygen conveyance and absorption into the molten pool. Therefore, the oxygen content in the weld metal remains nearly constant at around 200 ppm as shown in Fig. 1. Because the heavy oxide layer is continuous at the periphery area on the weld pool surface, the liquid pool/oxide layer interface is present instead of the liquid pool/gas surface. In this case, the Marangoni convection by the liquid pool surface tension at the periphery area is no longer the main factor. However, in the pool center area, the inward Marangoni convection still exists because there is no oxide layer on the pool center as shown in Fig. 6(c). This inward convection transports the hot liquid melt at the center of the weld pool from the surface to the bottom. As a result, the weld shape will become wide with a concave bottom as shown in Fig. 2(e, f, E and F).

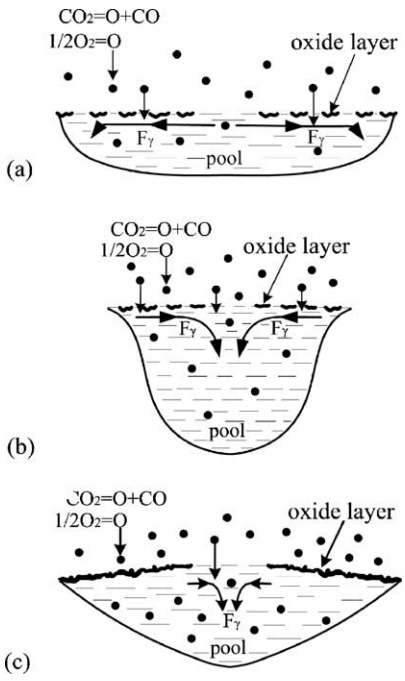

Fig. 6. Model for liquid pool convection and oxide layer behavior.

4. Conclusions

Small addition of O_2 or CO_2 to the argon shielding gas provides a means of controlling the weld metal oxygen content. Oxygen and carbon dioxide in the shielding gas have nearly the same effect on the oxygen absorption into the molten pool when their concentration in shielding gas is below 1.0 vol.%. When the O_2 or CO_2 concentrations in shielding gas are in the range of 0.3 vol.%–0.5 vol.%, a deep and narrow weld shape occurs and the weld D/W ratio is over 0.5.

The oxygen content in the weld metal is the main factor controlling the Marangoni convection mode for the liquid SUS304 stainless steel weld pool in the GTA welding process. When the weld metal oxygen content is over the critical value of 100 ppm, the Marangoni convection changes from suddenly an outward model to an inward model, and ultimately, the weld pool varies from a wide shallow shape to narrow deep shape.

Based on thermodynamic calculations and the experimental analysis to the weld metal oxygen content, Cr_2O_3 and SiO_2 oxides possibly form at the periphery area on liquid pool surface under the arc column. A continuous heavy oxide layer covers at the periphery area of liquid pool surface when the oxygen or carbon dioxide concentration in the shielding gas is over 0.6 vol.%. This heavy oxide layer is a barrier for the oxygen dissolution. Also the liquid pool/oxide layer interface is instead of the liquid pool/gas surface, and the Marangoni convection at the periphery area is no longer a main driving force.

Small addition of O_2 or CO_2 to the argon shielding gas can significantly increase the weld penetration. The effective range for both the O_2 and CO_2 concentrations for deep penetration is the same because of the low oxidizing gas additions to the argon shielding gas and the significant dissociation reactions of O_2 and CO_2 in the high temperature arc plasma column. The limited dissolution of oxygen in the welding process and the heavy oxide layer on the weld pool make the weld metal oxygen remained constant around 200 ppm–250 ppm when the O_2 or CO_2 concentration is over 0.6 vol.%.

Acknowledgements

This work is the result of "Development of Highly Efficient and Reliable Welding Technology", which is supported by the New Energy and Industrial Technology Development Organization (NEDO) through the Japan Space Utilization Promotion Center (JSUP) in the program of Ministry of Economy, Trade and Industry (METI), 21st Century COE Program, ISIJ research promotion grant and JFE 21st Century Foundation grant.

References

[1] S. Kou, Welding Metallurgy, Wiley, 1987, p. 91.
[2] B.E. Paton, Avtom. Svarkal. 6 (1974) 1.
[3] W.S. Bennett, G.S. Mills, Weld. J. 53 (1974) 548s.
[4] W.F. Savage, E.F. Nippes, G.M. Goodwin, Weld. J. 56 (1977) 126s.
[5] C.R. Heiple, J.R. Roper, Weld. J. 60 (1981) 143s.
[6] Y. Takeuchi, R. Takagi, T. Shinoda, Weld. J. 71 (1992) 283s.
[7] M. Tanaka, T. Shimizu, H. Terasaki, M. Ushio, F. Koshi-ishi, C.-L. Yang, Sci. Technol. Weld. Join. 5 (2000) 397.
[8] M. Kuo, Z. Sun, D. Pan, Sci. Technol. Weld. Join. 6 (2001) 17.
[9] D.S. Howse, W. Lucas, Sci. Technol. Weld. Join. 5 (2000) 189.
[10] C.R. Heiple, J.R. Roper, Weld. J. 61 (1982) 97s.
[11] W. Lucas, D. Howse, Weld. Met. Fabri. 64 (1996) 11.
[12] D.D. Schwemmer, D.L. Williamson, Weld. J. 58 (1979) 153s.
[13] T. Lpaskell, C. Lundin, H. Castner, Weld. J. 76 (1997) 57.
[14] Y. Wang, H.L. Tsai, Metall. Mater. Trans. 32B (2001) 501.
[15] S.P. Lu, H. Fujii, H. Sugiyama, K. Nogi, Metall. Mater. Trans. 34A (2003) 1901.
[16] B.N. Bad'yanov, Avtom. Svarka. 1 (1975) 74.
[17] C.R. Heiple, P. Burgardt, Weld. J. 64 (1985) 159s.
[18] T. Kuwana, Y. Sato, Trans. Jpn. Weld. Soc. 17 (1986) 124.
[19] T. Kuwana, Y. Sato, Trans. Jpn. Weld. Soc. 19 (1988) 134.
[20] T. Kuwana, Y. Sato, Q. J. Jpn. Weld. Soc. 7 (1989) 43.
[21] T. Kuwana, Y. Sato, Q. J. Jpn. Weld. Soc. 7 (1989) 49.
[22] T. Kuwana, Y. Sato, Q. J Weld. Soc. 7 (1989) 330.
[23] T. Kuwana, Y. Sato, A. Otobe, H. Ohnishi, Q. J. of Japan Weld. Soc. 8 (1990) 91.
[24] Y. Sato, K. Tomita, T. Kuwama, Q. J. Jpn. Weld. Soc. 10 (1992) 384.
[25] Y. Sato, T. Kuwana, ISIJ Int. 35 (1995) 1162.
[26] T. Kuwana, Y. Sato, N. Onodera, Q. J. Jpn. Weld. Soc. 9 (1991) 410.
[27] T.A. Palmer, T. DerRoy, Weld. J. 75 (1996) 197s.
[28] Y. Sato, W. Dong, H. Kokawa, T. Kuwana, ISIJ Int. 40 Suppl, 2000 p.S20.
[29] H. Kokawa, Trans. Jpn. Weld. Soc. 72 (2003) 414.
[30] H. Wada, R.D. Pehlke, Metall. Trans. 8B (1977) 675.
[31] W. Dong, H. Kokawa, Y. Sato, S. Tsukamoto, Metall. Mater. Trans. 34B (2003) 75.
[32] M. Uda, S. Ohno, T. Wada, Trans. Jpn. Weld. Soc. 38 (1969) 382.
[33] J.D. Katz, T.B. King, Metall. Trans. 20B (1989) 175.
[34] T.A. Palmer, T. DebRoy, Sci. Technol. Weld. Join. 3 (1998) 190.
[35] H. Taimatsu, K. Nogi, K. Ogino, J. High Temp. Soc. 18 (1992) 14.
[36] S.P. Lu, H. Fujii, H. Sugiyama, M. Tanaka, K. Nogi, Mater. Trans. 43 (2002) 2926.
[37] T. Zacharia, S.A. David, J.M. Vitek, T. Debroy, Weld. J. 68 (1989) 499s.